Characterizing the Susceptibility Calibration Factor in Heterogeneous Vascular Networks

Natenael B Semmineh[1], Junzhong Xu[2], and C Chad Quarles[3]

[1]*institute of imaging science, Vanderbilt University, nashville, TN, United States,* [2]*Vanderbilt University,* [3]*institute of Imaging science, Vanderbilt University, Nasville, TN*

Introduction: A central assumption in all DSC-MRI studies is that a linear relationship, with a spatially uniform rate constant termed the vascular susceptibility calibration factor (k_p), exists between the contrast agent (CA) concentration and the measured transverse relaxation rate change. Normal tissue vascular networks display an ordered structure, while the tumor microvasculature has a disordered and tangled structure, with a large degree of random variation in vessel length and diameter, and branching patterns. Given the dependence of susceptibility field gradients on vascular geometry this assumption could significantly impact the reliability of DSC-MRI hemodynamic measurements. We propose the use of an efficient computational approach that combines the finite perturber method (FPM) [1] with the finite difference method (FDM) [2] in order to estimate the vascular susceptibility calibration factor for arbitrary vascular tree networks simulated to replicate structural properties observed in normal and tumor tissue.

Methods: To simulate susceptibility contrast induced by compartmentalization of CA with arbitrary shaped vascular network, we developed and validated an efficient computational approach that combines the FPM with the FDM, which we term the Finite Perturber Finite Difference Method (FPFDM) [3]. We constructed model vascular network using a fractal tree model [4]. Starting with an initial cylindrical segment representing an arterial vessel, the vascular tree is created using bifurcation and trifurcation at each junction into smaller daughter segments. For this study a target vascular volume fraction (6%) is set to terminate the fractal tree development.

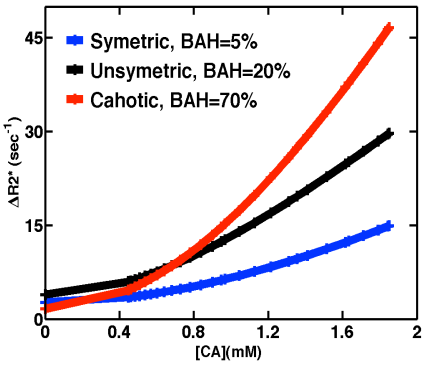

Figure 3: ΔR_2^* dependence on [CA] for three different vascular

At a junction the diameter of each daughter vessels is calculated using the "square law" [5] and given some degree of randomness along with the branching angles to create tumor like heterogeneous structures. The dependence of ΔR_2^* on vascular CA concentration curve is used to compute the K_p values for each simulated tissue.

Vascular volume fraction= 6%

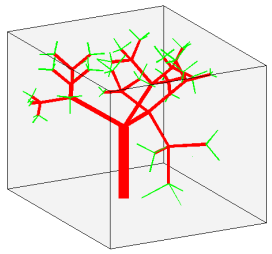

Figure 1: Example of symmetric vascular structure

Vascular volume fraction= 6%

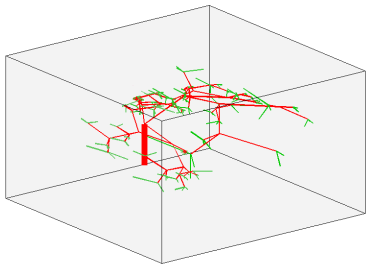

Figure 2: Example of chaotic vascular structure

Results: **Figure 1** shows an example symmetric vascular tree with homogenous branching and rotation angles as well as bifurcation index (α), which measures the relative diameter of the branches as compared to the parent cylinder. The heterogeneous nature of the tumor vascular structure is represented in **Figure 2**. The dependence of ΔR_2^* on CA concentration for a typical DSC-MRI bolus injection is shown in **Figure 3** for three different tissue structures characterized by their α variation among branches and branching angle heterogeneity (BAH), which is allowed to vary up to 70% in this simulation. Using the ΔR_2^* vs [CA] curves k_p values ranging from 7-28 $(mM\text{-}sec)^{-1}$ was obtained. The k_p values for tumor tissues were higher that the normal tissue, up to four fold for this particular simulation.

Conclusion: The computational results presented herein show marked k_p heterogeneity across tissue samples, suggesting that the assumption of a constant k_p for all tissue types could affect the reliability of DSC-MRI derived perfusion parameters. Currently a more stringent study is under way to further characterize the k_p for simulated vascular trees and μCT based tissue angiograms.

Reference: [1] Pathak A P, et al. NeuroImage 40 2008; 1130–1143. [2] Junzhong Xu, et al. Phys Med Biol. 2007; 52(7):N111-26. [3] Semmineh S., et al., ISMRM 2010. [4] E. Sabo, et al Clin Cancer Res, vol. 7, no. 3, pp. 533–7, Mar 2001. [5] M. Zamir, J. Theor. Biol., vol. 197, no. 4, pp. 517–526, 1999.[6] Pathak A P, et al. J. MRI 8:397–403 (2003).

Acknowledgements: NCI R00 CA127599, NCI P30 CA068485, NCI U24 CA126588